

カセンサとカメラのセンサフュージョンに基づいた コンクリート構造物の欠陥検出*

ルイ笠原純ユネス** 湊真司*** モロアレッサンドロ† 禹ハンウル*** 山下淳** 浅間一**

Defect Detection in Concrete Structures Using Sensor Fusion of Force Sensor and Camera

Jun Younes LOUHI KASAHARA, Shinji MINATO, Alessandro MORO, Hanwool WOO, Atsushi YAMASHITA and Hajime ASAMA

Inspection of concrete structures such as tunnels and bridges is most often performed in outdoor environments where wind and vehicle noise are strongly present. Therefore, inspection methods must be robust against acoustic noise. The use of an impact hammer, which has a force sensor embedded in its head, has the advantage of being inherently robust against acoustic noise compared to the commonly used acoustic hammering inspection method while retaining the same ease of use. However, being able to capture data only during the short impact time, force sensor alone does not allow for acceptable defect detection. Therefore, in this study, the detection performance of defects was improved by considering the position of the crack on the concrete surface and the sample position obtained from a camera image in addition to the response of the force sensor of the impact hammer. From the experimental results obtained using concrete test blocks in laboratory conditions, the ability to detect defects with an impact hammer was significantly improved.

Key words: defect detection, sensor fusion, force sensor, computer vision, clustering

1. Introduction

In Japan, a high economic growth period roughly between 1960 and 1980 enabled the construction of a large number of social infrastructures such as tunnels and bridges. Those are predominantly made of concrete and it is expected that their deterioration will accelerate in the upcoming 20 years. Therefore, the inspection of concrete social infrastructures is gaining focus, especially in light of disastrous events such as the collapse of the Sasago tunnel¹⁾.

Current methods used for the inspection of concrete structures are largely manual, i.e., they require human operators. Such methods have the drawback of being highly dependent on the skill of human operators. Moreover, due to the aging of the population, the number of available human operators is also declining. Therefore the automatic inspection of concrete structures is highly desirable.

There are several non-destructive testing methods for inspection of concrete structures²⁾. Among those dealing with detecting defects beneath the surface, thermographic methods, electromagnetic methods and stress wave propagation methods are the most popular. Thermographic methods use infrared cameras and the difference in thermal conductivity of defects for detection³⁾. Electromagnetic methods use the response to high frequency pulses to scan portions of the concrete⁴⁾. Stress wave propagation methods use the response to mechanical stress induced to the concrete, usually from an impact.

One of the most used inspection methods for concrete structure is the hammering test, a stress wave propagation method, shown



Fig.1 A human operator conducting the hammering test on the wall portion of a tunnel.

in Fig. 1. It consists in a human operator hitting the surface of the structure with a hammer and assessing the presence of defects beneath the surface from the returned impact sound. Compared to a simple visual inspection, the hammering test allows to detect defects beneath the surface and therefore, allows to determine the propagation direction of the defect beneath the surface. This is critical since several defects propagating beneath the surface towards the same point present an increased risk of peeling, i.e., a large concrete slab falling from the structure. Compared to other inspection methods, the hammering test has the advantage of versatility and simplicity. No heavy equipment is needed and sensors are not required to be in contact with the concrete, which allows for very fast inspection of large structures.

Some previous works focused on the pressure characteristics of the hammering sound⁵⁾ or direct methods⁶⁾, focusing primarily on data visualization and integration into a comprehensive inspection environment with several sensors. However, the majority of

* 原稿受付 令和2年6月29日

掲載決定 令和2年7月15日

** 正会員 東京大学(〒113-8656 東京都文京区本郷7-3-1)

*** 東京大学

† ライテックス(〒190-0023 東京都立川市柴崎町3-5-11)

them explored machine learning approaches such as ⁷⁾ with Linear Prediction Coefficients, ⁸⁾ with Neural Networks, ⁹⁾ with Ensemble Learning, ¹⁰⁾¹¹⁾ with Clustering. However, since sound is used as input data, the decrease in accuracy in the presence of acoustic noise is an issue: concrete structures inspection sites are located in outdoor environments and a fair amount of acoustic noise resulting from winds and vehicular traffic can be expected.

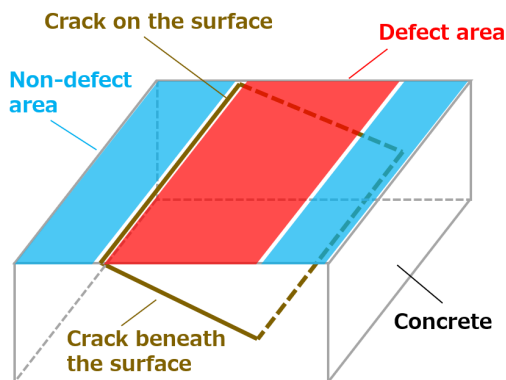
Therefore, in this study is considered the use of impact hammer for the inspection of concrete structures. This type of hammer possesses a force sensor embedded in its head and allows to monitor the force feedback during hammering. This allows inherent robustness against acoustic noise.

The objective of the present paper is to detect defects in concrete structures using sensor fusion between a force sensor and a camera. During the analysis of the force sensor data, the visible crack position information obtained from the camera is used conjointly with the position information of each sample in order to propagate information from easily detected defect samples in the vicinity of the visible crack.

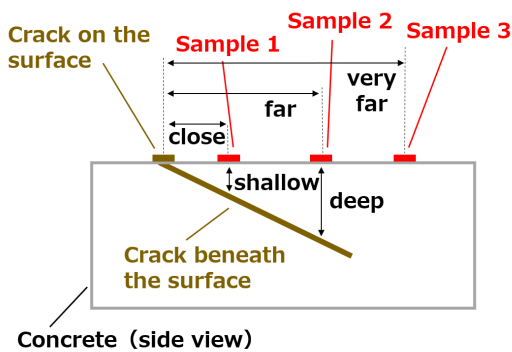
2. Method

2.1 Concept

One challenging aspect of data collected by an impact hammer is its shortness. Indeed, the impact hammer provides much less effective data volume for defect detection compared to the hammering



(a) Defect areas are characterized as cracks running beneath the surface.



(b) Side view of the considered concrete portion.

Fig.2 Concept of the proposed method. Samples close to the visible crack and easy to detect are used in order to boost the detection of defect samples further away from the crack, which are deep and more difficult to detect.

test. The hammering test is based on audio segments with a duration of about 23 ms each ¹¹⁾ while the impact hammer, allowing only to provide signal related to the concrete characteristics during the immediate moments of impact, is effective only for about 0.2 ms from our experience. The amount of valid data differs by more than 100 times in terms of time. Therefore, it is desirable to supplement information necessary for detecting defects by adding information from other sources.

There are several additional information that can be considered. Those would be for example the impact sound of the impact hammer, the image of the concrete surface, or the three-dimensional shape ¹²⁾ of the concrete surface. However, as stated earlier, acoustic information presents the drawback of being susceptible to acoustic noise, a troublesome point in the expected outdoor inspection sites. Obtaining three-dimensional shape measurements requires precise installation of laser devices, hindering the ease of use and high practicability of using an impact hammer. Therefore, in this study is considered the use of the image of the concrete surface, i.e., visual information obtained from a camera, to complement information from the impact hammer. Visual information is an important part of the inspection process and allows the detection of portions of defects visible from the surface, i.e., cracks, and can provide critical information ¹¹⁾¹³⁾.

In Fig. 2(a) is shown the locations of defect and non-defect areas in a considered portion of a concrete structure. A visible defect, i.e., crack, is present on the surface. In Fig. 2(b) is shown a side view of that same concrete portion. Considering samples 1, 2 and 3 in Fig. 2(b), corresponding to different hit locations on the concrete, samples 1 and 2 are defects and sample 3 is a non-defect. Sample 1 is shallow and can be expected to be easy to detect. Sample 2 is deep and difficult to detect. Those two samples are also characterized by their distance from the crack on the surface, close and far, respectively. The concept of the proposed method is to make use of the crack position on the surface obtained using a camera in order to propagate information on defects from samples close to visible cracks to samples far from visible cracks.

2.2 Overview of Proposed Method

Figure 3 shows the processing flow of the proposed method.

First, multiple points on the concrete surface are hit with an impact hammer and the response of force sensor located on its head is recorded for each sample. In addition, the position information

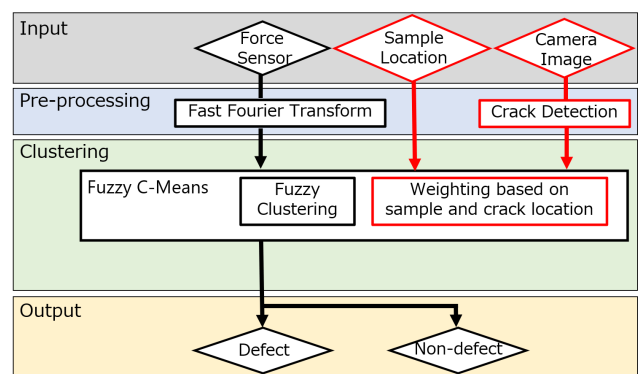


Fig.3 Overview of proposed method.

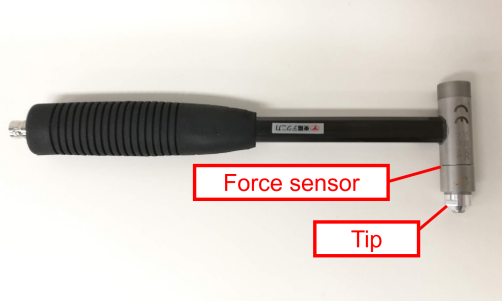


Fig.4 Impact hammer model 086C03 from PCB Piezotronics. A force sensor is embedded in the hammer head and protected by a tip, which is the point of contact with the concrete surface during the hammering test.

of the crack on the concrete surface is obtained by performing image processing on the camera image. Next, the force sensor data is converted to Fourier spectrum using Fast Fourier Transform. This is used as feature vector for the following analysis. Finally, using a modified Fuzzy C-Means algorithm, samples are clustered into defects and non-defects.

2.3 Impact Hammer

The used impact hammer is shown in Fig. 4.

The hammer head has a built-in piezoelectric element force sensor made of quartz or ceramic. When a structure is hit using an impact hammer, the force signal at the time of contact can be measured from the response of the force sensor: this force sensor converts an external force into a voltage by utilizing the polarizing property of the piezoelectric element in proportion to mechanical pressure.

Therefore, from the response of the force sensor, a time-series data of the contact force when the concrete surface is hit with the impact hammer can be collected.

Traditionally, the impact hammer is used conjointly with accelerators secured onto the surface of the tested concrete structure relatively close to the impact point in order to conduct modal analysis¹⁴⁾. However, having to secure sensors onto the surface of the concrete is a tedious task which is not suited for the inspection of large-scale structures such as those considered in this paper. Furthermore, this would involve adhesives which would require thorough clean-up of the inspected surface in order not to hinder visual inspections, lengthening the inspection time. Therefore, in the present study, the impact hammer without any additional sensor secured on the concrete surface is considered for defect detection in concrete structures.

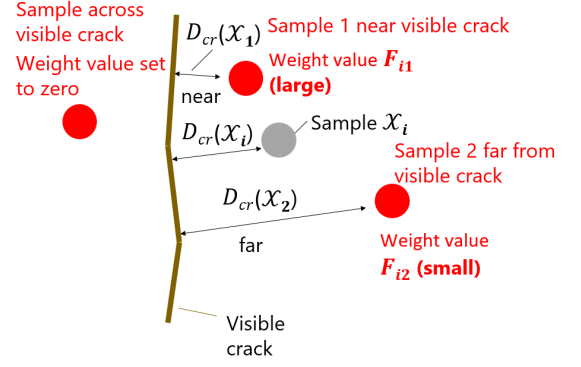
2.4 Crack Position Detection Using Computer Vision

In this study, cracks were detected by performing threshold processing on camera images.

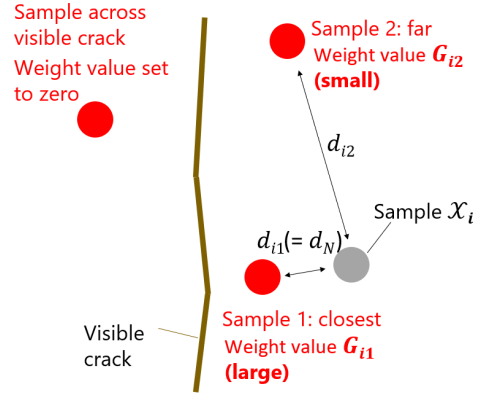
First, the concrete RGB image obtained from the camera is converted to a grayscale image. Next, the luminance value $\text{src}(x, y)$ at the coordinates (x, y) of the obtained grayscale image is classified into two values based on a manually set threshold value T_c .

$\text{dst}(x, y)$, which is the final luminance value at the coordinates (x, y) of the binarized image, can be obtained by Eq. (1):

$$\text{dst}(x, y) = \begin{cases} 255, & \text{if } \text{src}(x, y) > T_c \\ 0, & \text{otherwise} \end{cases} . \quad (1)$$



(a) Weighting based on crack and distance between samples.



(b) Weighting based on distance between samples.

Fig.5 Illustration of the proposed weighting system.

Since the crack has a lower brightness than the healthy part, the place where the luminance value $\text{dst}(x, y)$ is 0 is defined as the crack.

2.5 Feature Vector Extraction

The considered dataset is composed of N impact hammer samples, corresponding each to one hammer strike on one location of the tested concrete structure. Using Fast Fourier Transform, the dataset of time-series force sensor samples $\{\mathcal{X}_i\}_{i=1, \dots, N}$ is transformed into Fourier Spectrums $\{\mathbf{x}_i\}_{i=1, \dots, N}$.

2.6 Clustering

Separation of samples between defect and non-defect is conducted using Fuzzy C-Means. Fuzzy C-Means is a fuzzy clustering algorithm, meaning that samples belong to several clusters at the same time but with varying degrees, which are expressed through fuzzy membership coefficients $\{u_{ij}\}_{i \in [1 \dots N], j \in [1 \dots K]}$. Fuzzy membership coefficient u_{ij} indicates how strongly the i th sample belongs to the j th cluster¹⁵⁾.

First, initial cluster centers, or *seeds*, are randomly chosen among the dataset. Then, update phases are conducted until a chosen termination criterion for convergence is met. This update phase is composed of fuzzy membership update and centroid update steps.

The fuzzy membership update step itself is first computed as in Eq. (2), where K is the given number of clusters, $\{\mathbf{c}_j\}_{j \in [1 \dots K]}$ cluster centers and m a parameter controlling the fuzzyness of the

system. It is worth noting that this only concerns force sensor data.

$$u_{ij} = \left[\sum_{l=1}^K \left(\frac{\|\mathbf{x}_i - \mathbf{c}_j\|}{\|\mathbf{x}_i - \mathbf{c}_l\|} \right)^{2/(m-1)} \right]^{-1}. \quad (2)$$

The crack position information obtained following the process described in Section 2.4 is incorporated into the clustering process via a weighting system using an estimator $\{h_{ij}\}_{i \in [1 \dots N], j \in [1 \dots K]}$, as in Eq. (3). This estimator basically computes what the fuzzy membership of a sample should be according to its neighbors in SS . This neighborhood is computed based on both crack position and position information of samples on the tested structure. For sample \mathcal{X}_i , $SS(\mathcal{X}_i)$ corresponds to samples belonging on the same side of the visible crack.

$$h_{ij} = \sum_{k \in SS(\mathcal{X}_i)} W_{ik} u_{kj}. \quad (3)$$

The estimator and the fuzzy membership coefficients computed on the force sensor data are then combined following Eq. (4), with p and q parameters controlling the contribution of each source.

$$u'_{ij} = \frac{u_{ij}^p h_{ij}^q}{\sum_{l=1}^K u_{il}^p h_{il}^q}. \quad (4)$$

Once convergence has been reached, conversion to crisp clustering is conducted by maximum membership.

2.7 Proposed Weighting System

The proposed weight system W_{ik} in (3) is determined by the product of two functions F_{ik} and G_{ik} , as in Eq. (5).

$$W_{ik} = \frac{F_{ik} G_{ik}}{\sum_{l \in SS(\mathbf{x}_i)} F_{il} G_{il}}. \quad (5)$$

The concept of the proposed method is that a sample closer to the visible crack is more likely to be correctly recognized as a defect. This is reflected through F_{ik} , as in Eq. (6):

$$F_{ik} = \begin{cases} \left(\frac{D_{cr}(\mathcal{X}_i)}{D_{cr}(\mathcal{X}_k)} \right)^\alpha, & \text{if } D_{cr}(\mathcal{X}_i) < \frac{1}{2}D \\ \left(\frac{D_{cr}(\mathcal{X}_i)}{D_{cr}(\mathcal{X}_k)} \right)^{-\alpha}, & \text{otherwise} \end{cases} \quad (6)$$

$D_{cr}(\mathcal{X}_i)$ and $D_{cr}(\mathcal{X}_k)$ are the shortest distance to crack of samples \mathcal{X}_i and \mathcal{X}_k , respectively. Parameter α is a constant defining how strong is the propagation of information. D is the dimension of the tested area, which corresponds, assuming the inspection area has been narrowed down to a square centered on the crack visible from the surface, to the length of the tested area.

As shown in **Fig. 5(a)**, given the considered sample \mathcal{X}_i , the distance to visible crack D_{cr} is computed for other samples located in the same side of the visible crack. For example, Sample 1 and Sample 2 in **Fig. 5(a)** are located near and far from the visible crack, respectively. Therefore, Sample 1 having a higher probability of being correctly detected, F_{i1} has a larger weight than F_{i2} . However, as the sample \mathcal{X}_i is farther from the crack, the possibility that the sample \mathcal{X}_i is a defect decreases. This is reflected by the strength of the surrounding weights decreasing.

The same principle is applicable to very far samples from visible cracks, which are very likely to be non-defects. Therefore, past half the dimension of the tested area, the tendency described earlier is reversed by inversion of the ratio defining F_{ik} .

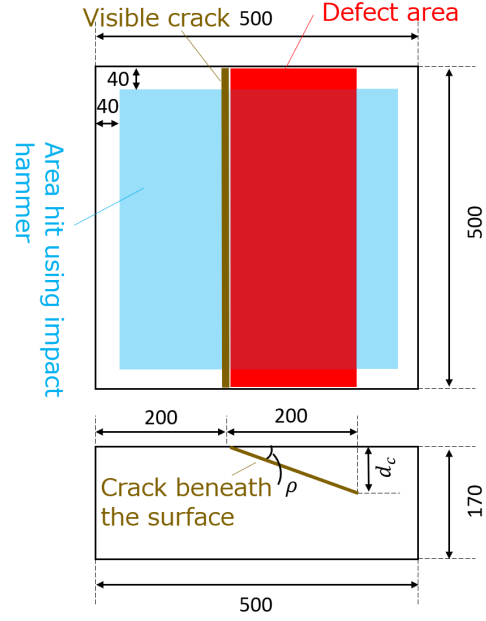


Fig. 6 Generic schematic of the considered concrete test blocks. Dimensions in mm.

Table 1 Characteristics of the considered concrete test blocks.

	Block A	Block B
Crack angle ρ (deg.)	15	30
Deepest defect d_c (mm)	53.6	115.5

Samples which are located close together on the surface of the tested area are more likely to belong to the same class. This is reflected through G_{ik} , a function designed to perform increased weighting as the distance between samples becomes shorter.

G_{ik} is defined as in Eq. (7), with $d_{i,k}$ the distance between sample \mathcal{X}_i and the surrounding sample \mathcal{X}_k , d_N the distance of the closest sample to \mathcal{X}_i and σ a constant.

$$G_{ik} = \frac{1}{\sqrt{2\pi}\sigma} \exp \left\{ - \left(\frac{d_{i,k}}{d_N} \right)^2 / 2\sigma^2 \right\}. \quad (7)$$

Figure 5(b) shows a schematic of the positional relationship between samples. Sample 1 is closer to sample \mathcal{X}_i than sample 2, therefore G_{i1} has a larger weight than G_{i2} . Since sample 1 is the nearest neighbor of sample \mathcal{X}_i , d_{i1} is defined as d_N . As for F_{ik} , samples on the other side of the crack are excluded from the weighting.

3. Experiments

Experiments were conducted in laboratory conditions using concrete test blocks. Those contain defects with precisely known characteristics thanks to elaborate fabrication process.

A generic schematic of the tested concrete test blocks is shown in **Fig. 6**. Two blocks, Block A and Block B, were considered and their characteristics are reported in **Table 1**. Both were hit at 225 locations following a regular grid for 105 non-defect samples and 120 defect samples. This grid was used to acquire the location of each sample. Collecting samples on the edge of the concrete blocks was not done in order to avoid different border con-

ditions. The used impact hammer was a model 086C03 from PCB Piezotronics (weight 160g, length 216mm, head diameter 15.7mm, sensitivity 2.25 mV/N, peak force range $\pm 2224\text{N}$ ^{*1}). Force sensor data was recorded using a data logger at the maximum frequency of 105,469Hz in order to obtain as much data as possible during the short impact time. T_c was manually tweaked around a value of 100 for best output. Parameters were set as $m = 2$, $p = 1$, $q = 1.3$, $\alpha = 6$, $\sigma = 0.8$ and D was set to the size of the blocks, at 500mm.

Experiments were conducted with the following methods:

1. (A) K-Means clustering.
2. (B) Spectral Clustering as described in ¹⁶.
3. (C) The method of ¹¹ adapted for use with force sensor data, i.e., without Mel Frequency Cepstrum Coefficients (MFCC).
4. (D) The proposed method.

The performance of each method was evaluated using the Rand index ¹⁷, a common performance measure of clustering ranging between 0 and 1, with the higher value indicating the better method.

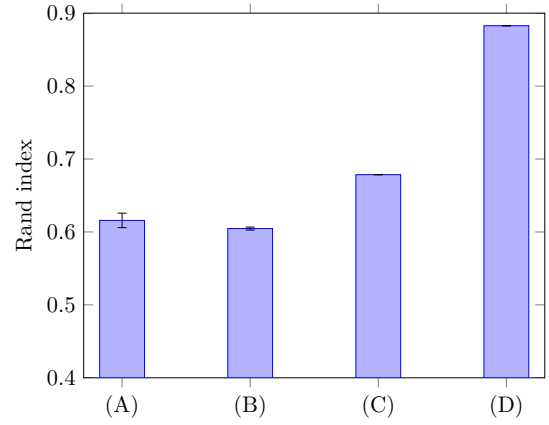
4. Results and Discussions

The average performance obtained are reported in Fig. 7. Additionally, in Figs. 8, 9 and 10 are shown pictures of concrete test blocks, the outputs of the crack detection, the outputs of the method of ¹¹ and the outputs of the proposed method for Block A and Block B, respectively.

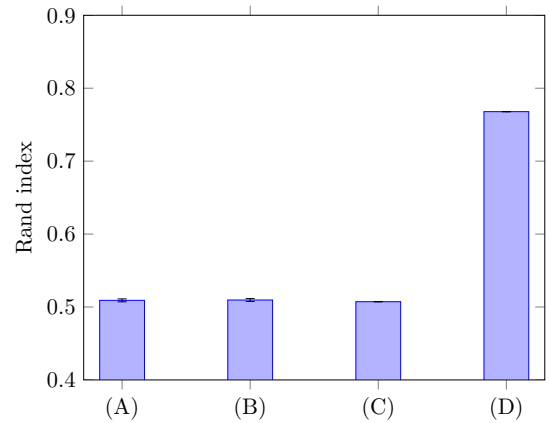
It can be first noticed in Fig. 7 that performance for all methods are lower for Block B than for Block A. This is because the defect in Block B is deeper than in Block A: 53.6mm at the deepest point for Block A against 115.5mm for Block B. Deeper defects are more difficult to detect since the thickness of the concrete portion over the crack increases and becomes similar to non-defect concrete. However, deeper defects can be considered more dangerous since they can potentially result in the peeling off of much larger amounts of concrete if left unchecked.

Performance of both K-Means and Spectral Clustering for both blocks were closely similar. While some defects were corrected detected on Block A, the results on the more difficult Block B were disappointing.

The method of ¹¹ was adapted here for use with force sensor data, i.e., the MFCC transformation was omitted since it is only applicable to acoustic data. While this method still exhibited good performance on Block A, outperforming K-Means and Spectral Clustering, it failed as well on Block B. This is certainly due to the fact that a large part of the performance of the method of ¹¹ is based on the use of MFCC, as shown in ¹⁸. The method of ¹¹ incorporates a weighting system in Fuzzy C-Means similar to our proposed method, also using sample position but not using crack position. This explains the better performance it managed to obtain compared to K-Means on Block A: in Fig. 9(c) it can be seen that clusters are much more spatially compact and localized. How-



(a) Average performance on Block A.



(b) Average performance on Block B.

Fig.7 Performance of K-Means (A), Spectral Clustering (B) ¹⁶, method of ¹¹ (C) and the proposed method (D) on the considered concrete test blocks. Average performance over 20 runs are reported. Error bars corresponds to 1 standard deviation.

ever, the limits of this method are apparent on Block B, shown in Fig. 10(c), where almost no improvement over K-Means' output, shown in Fig. 10(b), can be seen except a slightly increased compacity of defect and non-defect areas.

The proposed method achieved the highest performance on both Block A and Block B. It can be seen in Figs. 8(b) and 8(d) that the visible cracks were correctly detected for both Block A and Block B. The proposed method outperforming the method of ¹¹ indicates the advantages provided by the inclusion of crack position in the weight system during the clustering by Fuzzy C-Means. On Block A it managed to detect more defect samples thanks to the increased influence from easy to detect defects. The method of ¹¹ on Block A, shown in Fig. 9(c), had several undetected defect samples on the upper defect area. Those were successfully detected using the proposed method, as shown in Fig. 9(d). The propagation of defect information enabled by our proposed method can be observed: a clear tendency to correctly detect samples on a single side of a crack is noticeable.

This is even more apparent on Block B, where it managed to tip the balance from a detection failure in Fig. 10(c) to the output in Fig. 10(d). Here, while there is an overspill on the non-defect area, the output is much more in line with the ground truth of defects.

^{*1} The complete specifications for the impact hammer can be found at <https://www.pcb.com/products?m=086C03>

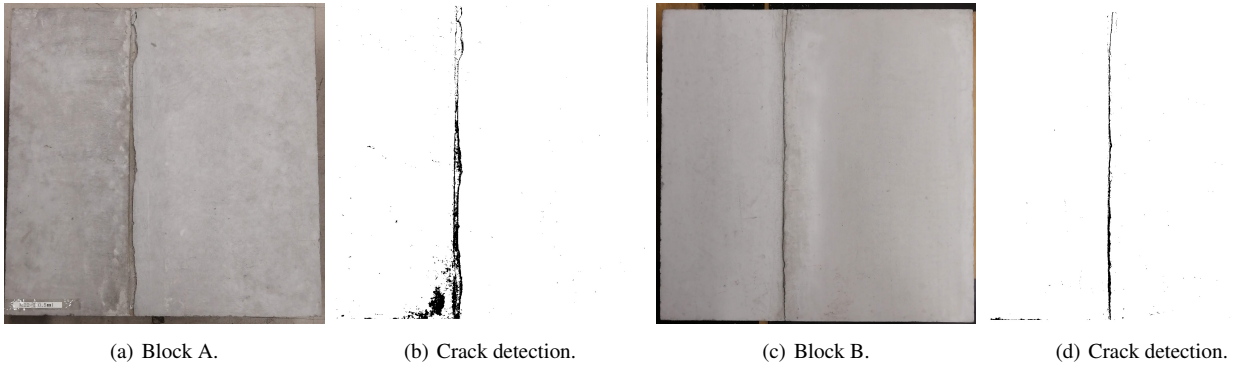


Fig.8 Crack detection outputs of the proposed method on the considered concrete test blocks.

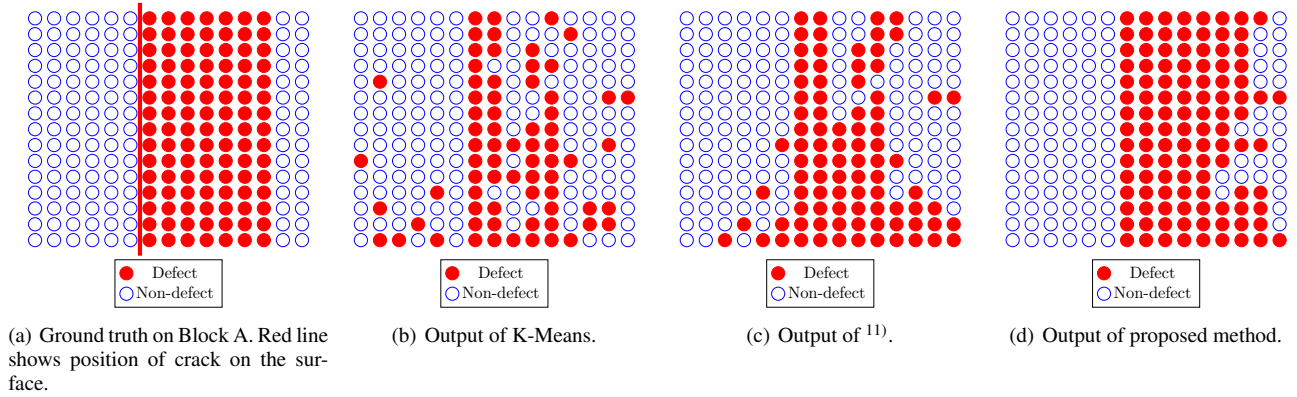


Fig.9 Example outputs on Block A.

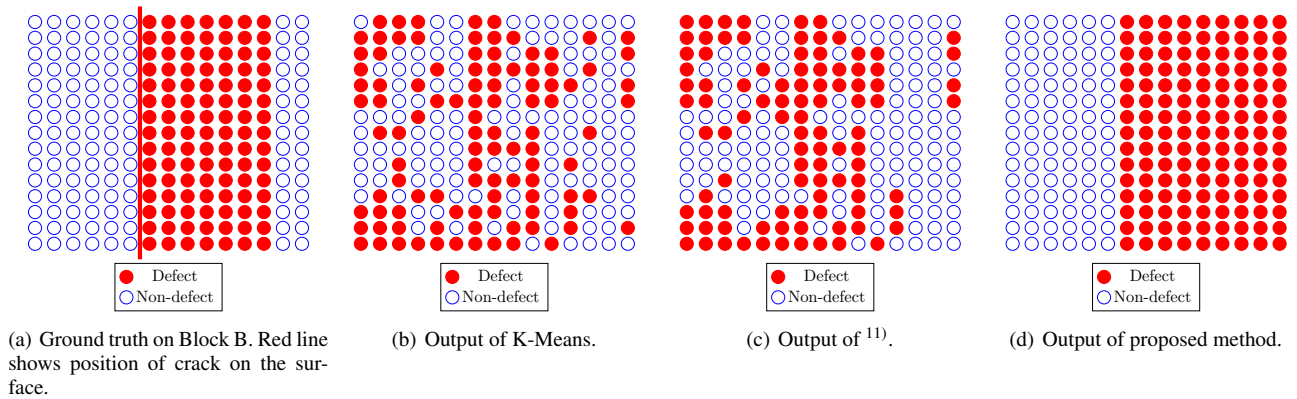


Fig.10 Example outputs on Block B.

This overspill can be attributed to the small right-side non-defect area size, which did not allow to present enough difference not to be assimilated into the defect cluster.

5. Conclusion

In the present paper, defect detection in concrete structures using sensor fusion between a force sensor and a camera was proposed. The proposed method allowed defect detection with a force sensor, with its inherent robustness to acoustic noise, with high performance. Visual information from the camera was incorporated in the force sensor data analysis by extraction of the position of the visual crack and propagating the defect information from easily detected samples. Experiments using concrete test blocks showed that the proposed method has improved detection performance, especially on deep defects.

In the future, we would like first to conduct experiments with ad-

ditional, larger test blocks, to further investigate the effects of the overspill observed on Block B. Furthermore, we would like to conduct experiments in more realistic, field conditions. To this aim, we will improve the visual crack detection portion of our proposed method with more robust approaches, such as ¹⁹⁾ for example.

Acknowledgment

This work was supported in part by JSPS KAKENHI Grant Number 19J12391 and by the Japan Construction Information Center (JACIC) foundation. The authors thank Prof. Hiromitsu Fujii, Department of Advanced Robotics, Chiba Institute of Technology for his valuable help. The authors also thank the Institute of Technology, Tokyu Construction Co., Ltd. for their precious help and cooperation.

References

- 1) BBC News: Japan Sasago Tunnel Collapse Killed Nine, <https://www.bbc.com/news/world-asia-20576492>, (2012).
- 2) J. Hoła, J. Bień, Ł. Sadowski and K. Schabowicz: Non-destructive and Semi-destructive Diagnostics of Concrete Structures in Assessment of Their Durability, *Bulletin of the Polish Academy of Sciences Technical Sciences*, **63**, 1, (2015) 87.
- 3) C. Maierhofer, R. Arndt, M. Röllig, C. Rieck, A. Walther, H. Scheel and B. Hillemeier: Application of Impulse-Thermography for Non-destructive Assessment of Concrete Structures, *Cement and Concrete Composites*, **28**, 4, (2006) 393.
- 4) S. Hong, H. Wiggerhauser, R. Helmerich, B. Dong, P. Dong and F. Xing: Long-term Monitoring of Reinforcement Corrosion in Concrete using Ground Penetrating Radar, *Corrosion Science*, **114**, (2017) 123.
- 5) Y. Sonoda and Y. Fukui: A Basic Study on Hammering Tests of Deteriorated Concrete Structures, *Proceedings of Our World in Concrete and Structures*, (2010).
- 6) J. Kim, N. Gucunski, T.H. Duong and K. Dinh: Three-dimensional Visualization and Presentation of Bridge Deck Condition Based on Multiple NDE Data, *Journal of Infrastructure Systems*, **23**, 3, (2016).
- 7) M.E. Henderson, G.N. Dion and R.D. Costley: Acoustic Inspection of Concrete Bridge Decks, *Nondestructive Evaluation Techniques for Aging Infrastructures & Manufacturing*, **3587**, (1999) 219.
- 8) G. Zhang, R.S. Harichandran and P. Ramuhalli: An Automatic Impact-based Delamination Detection System for Concrete Bridge Decks, *NDT & E International*, **45**, 1, (2012) 120.
- 9) H. Fujii, A. Yamashita and H. Asama: Defect Detection with Estimation of Material Condition using Ensemble Learning for Hammering Test, *Proceedings of the International Conference on Robotics and Automation*, (2016) 3847.
- 10) J.Y. Louhi Kasahara, H. Fujii, A. Yamashita and H. Asama: Unsupervised Learning Approach to Automation of Hammering Test using Topological Information, *Robomech Journal*, **4**, 1, (2017) 13.
- 11) J.Y. Louhi Kasahara, H. Fujii, A. Yamashita and H. Asama: Fuzzy Clustering of Spatially Relevant Acoustic Data for Defect Detection, *Robotics and Automation Letters*, **3**, 3, (2018) 2616.
- 12) P. Giri and S. Kharkovsky: Dual-laser Integrated Microwave Imaging System for Nondestructive Testing of Construction Materials and Structures, *IEEE Transactions on Instrumentation and Measurement*, **67**, 6, (2018) 1329.
- 13) J.Y. Louhi Kasahara, A. Yamashita and H. Asama: Acoustic Inspection of Concrete Structures Using Active Weak Supervision and Visual Information, *Sensors*, **20**, 3, (2020).
- 14) H.S. Atamturktur, C.R. Gilligan and K.A. Salyards: Detection of Internal Defects in Concrete Members Using Global Vibration Characteristics, *ACI Materials Journal*, **110**, 5, (2013) 529.
- 15) J.C. Dunn: A Fuzzy Relative of the ISODATA Process and Its Use in Detecting Compact Well-separated Clusters, *Journal of Cybernetics*, **3**, 3, (1973), 32.
- 16) J. Shi and J. Malik: Normalized Cuts and Image Segmentation, *Transactions on Pattern Analysis and Machine Intelligence*, **22**, 8, (2000) 888.
- 17) W.M. Rand: Objective Criteria for the Evaluation of Clustering Methods, *Journal of the American Statistical Association*, **66**, 336, (1971) 846.
- 18) J.Y. Louhi Kasahara, H. Fujii, A. Yamashita and H. Asama: Clustering of Spatially Relevant Audio Data using Mel-Frequency Cepstrum for Diagnosis of Concrete Structure by Hammering Test, *Proceedings of the International Symposium on System Integration*, (2017) 787.
- 19) L. Zhang, F. Yang, Y.D. Zhang and Y.J. Zhu: Road Crack Detection Using Deep Convolutional Neural Network, *Proceedings of the International Conference on Image Processing*, (2016) 3708.